

# EVALUATION OF LOCAL & GLOBAL DUCTILITY RELATIONSHIPS FOR LOW-RISE MASONRY-INFILLED REINFORCED CONCRETE FRAME STRUCTURES

**R.K.L. Su, T.O. Tang & C.L. Lee**

*Department of Civil Engineering, The University of Hong Kong  
Pokfulam Road, Hong Kong, People's Republic of China*



## Summary

The paper presents the findings on a parametric study of the period lengthening effects of low-rise masonry-infilled reinforced concrete frame buildings using an incremental dynamic analysis (IDA). Simplified 2D building models utilizing Bouc-Wen model for describing strength, stiffness degradation and pinching effect were subjected to some selected ground motion records ranging from far to near field earthquakes in low to high seismicity regions. Simple equations correlating local to global ductilities derived from pushover (PO) analysis for buildings under soft storey failure mechanism are proposed. The equations take into account the governing factors like critical interstorey drift and number of storeys. The applicability of the equations was verified up to 7-storey buildings from the results of IDA. Such simple ductility relationships are likely to facilitate mostly the coefficient-based method, in which the typical PO analysis may be bypassed and allows making intuitive insight into the seismic performance of buildings.

**Keywords:** local, global ductility; coefficient-based method; confined masonry; soft storey; nonlinear analysis

## 1. INTRODUCTION

Damage state of a building is commonly expressed in terms of the interstorey drift ratio (IDR), defined as the ratio of the interstorey lateral displacement over the storey height. For low-rise masonry-infilled (MI) reinforced concrete (RC) frame buildings with uniform stiffness and lateral strength capacities along the building height, significant interstorey drifts are normally concentrated on the wall panels of the first storey of MI RC buildings when they are subjected to strong earthquakes. The soft storey failure mode is likely to occur at the ground level if the displacement or IDR demand exceeds the capacity.

Correlation between the period lengthening effect, related to global ductility ratio, and the local IDR is crucial to the seismic performance evaluation. For the low-rise MI RC buildings under soft storey mechanism with yield displacement known, if the performance level of deformation capacity of critical components (local ductility) can be identified through experimental or codified values, the global deformation capacity (global ductility) for an equivalent single-degree-of-freedom (SDOF) system can be specified. Alternatively, by defining the demands of global ductility ratio through coefficient-based method or the capacity spectrum method, the local deformation demands can then be worked out and compared with the capacity.

Such a simple ductility-based relationship is especially advantageous to facilitate the coefficient-based approach to serve as a rapid preliminary seismic performance assessment method for MI RC buildings without the requirement of onerous pushover (PO) analysis (FEMA 356, FEMA 440).

In the coefficient-based method proposed by different researchers (Miranda 1999, Gupta and Krawinkler 2000), Miranda used a drift factor  $\beta_2$  to express the ratio for maximum IDR ( $\theta_{max}$ ) to the roof drift ratio ( $\theta_{avg}$ ) under linear elastic state and a modified factor  $\beta_4$  to account for the concentration

of IDR during nonlinear state respectively. The simple expression of  $\beta_4$  obtained by regression of static PO analysis of the building models was based on the strong-column-weak-beam mechanism, which depends on three major factors comprising the number of storeys, failure mechanism and the local ductility. However, it is not applicable to buildings with soft storey mechanism and a high IDR demand at a particular storey.

Gupta and Krawinkler (2000) have developed a relationship between the inelastic interstorey drift demand and the 1<sup>st</sup> mode response spectral displacement of MDOF steel frame buildings by using several factors that account for the nonlinearity and the MDOF effects. The ratio of peak roof drift demands to interstorey drift demands have been found to be strongly dependent on the number of storeys and the ground motion characteristics. Constant median values of 1.2, 2.0 and 2.5 to 3.0 for low-rise, mid-rise and tall structures were suggested respectively under the buildings and earthquakes studied. The applicability of the correlation could be limited due to the possible variability of the degree of nonlinearity developed under earthquakes with different frequency contents.

Lee and Su (2012), Su *et al.* (2012) proposed a coefficient-based method to assess the inherent strength (spectral acceleration) of low-rise MI RC buildings under the soft storey mechanism. Drift related factors at the peak load state of low-rise MI RC buildings were calibrated by using the published experimental results for 2- to 5-storey buildings. However, the applicability of the method to 7-storey buildings and the theoretical correlation between the value of  $\theta_{max}$ , drift factors and the period lengthening factor ( $\beta$ ) have not been discussed in details.

In this article, simple expressions for correlating the local ductility factor with the global ductility factor for low-rise MI RC buildings with 3 to 7 storeys under soft storey mechanisms are proposed by the static PO analysis. The results are verified through the nonlinear time history analysis using the incremental dynamic analysis (IDA) performed under 10 accelerograms. The limitations of the study are also quantified.

## 2. DUCTILITY RELATIONSHIP

### 2.1. Existing Correlation for Low-rise MI RC Buildings

The response spectral displacement (RSD) for the equivalent SDOF, obtained from the PO curve of multiple-degree-of-freedom (MDOF) buildings, can be expressed in terms of the lateral roof displacement following the convention for Capacity Spectrum Method in ATC-40, or FEMA 356 as:

$$RSD = \frac{1}{\Gamma_1} \frac{\Delta_{roof}}{\phi_{roof,1}} \quad (2.1)$$

where  $\Gamma_1$  is the modal participation factor for the 1<sup>st</sup> vibration mode,  $\phi_{roof,1}$  is the normalised amplitude at the roof level of the 1<sup>st</sup> mode shape, and  $\Delta_{roof}$  is the actual lateral displacement at the roof. Such expression is still approximately correct for structures at inelastic state dominated by the 1<sup>st</sup> vibration mode, in which the global ductility for buildings under inelastic behaviour can be defined as:

$$\mu_G = \frac{RSD_{inel}}{RSD_y} = \frac{(\Delta_{roof})_{inel}}{(\Delta_{roof})_y} \quad (2.2)$$

where the subscripts  $y$  and *inel* refer to the yield state and inelastic state respectively.

For soft storey failure dictated by the lower strength capacity of either typical compression failure of diagonal strut, or the shear sliding failure of the mortar joint of infill resulting to knee-braced frame mechanism (Paulay and Priestley (1992)), the correlation of the local and global damage parameter can be expressed as follows.

With three major assumptions including linear deflection profile for yielding deformed shape; resultant of seismic lateral loading being acted at about  $2/3 H_b$  (effective height) for buildings with four or more

storeys, and the effective mass is lumped at the same effective height; and soft storey or inelastic displacement all concentrates at the first floor, Paulay and Priestley (1992) proposed a simplified correlation between the global ductility and the local ductility together with the number of storeys of the building as follows:

$$\mu_G = \frac{1}{n}(\mu_L - 1) + 1 \quad (2.3)$$

where  $n$  is the number of storeys, and  $\mu_L$  is the local ductility ratio of the critical storey level, which is usually the 1<sup>st</sup> storey due to soft storey mechanism.

Despite the fact that a compact formulation was derived, the applicability of the expression to MI RC buildings with different storeys was not studied in detail. The possible errors introduced by those assumptions were not clearly stated.

The coefficient-based assessment method was also adopted by Ruiz-García and Negrete (2009) for the seismic evaluation of MI RC buildings. The inelastic drift of the 1<sup>st</sup> storey was suggested to be estimated from the  $RSD_{inel}$  and the normalised participation factor assuming 1<sup>st</sup> mode of vibration dominates by PO analysis, with the MI RC buildings modelled as equivalent diagonal-strut models or wide-column models. The factor increases with the degree of damage level. Nevertheless, a simple correlation between the critical interstorey drift and  $RSD_{inel}$  was not included.

In view of low-to-moderate seismicity regions, where the MI RC buildings have a higher chance to survive in the earthquake primarily by its inherent strength but not relying on the unreliable post-peak inelastic deformation capacity (Su and Zhou 2009, Su *et al.* 2012), the drift related factors are likely to be determined in a more reliable manner by subjecting to limited inelastic deformation. Detailed investigation of the applicability of coefficient-based method to low-rise MI RC structures were conducted in Su and Zhou (2009), Lee and Su (2012), Su *et al.* (2012). Assuming no premature tearing failure of the floor diaphragms or tensile failure of tie columns due to insufficient steel reinforcement (Su *et al.* 2011), the inherent strength or the spectral acceleration of the MI RC buildings for relatively ductile sway mode of failure at a specific loading state can be determined as follows:

$$RSD = \frac{H_b \theta}{\lambda} \quad (2.4)$$

$$RSA = \frac{H_b}{T_0^2} \frac{(2\pi)^2}{\lambda} \frac{\theta}{\beta^2} \quad (2.5)$$

where  $\lambda$  is the drift factor;  $RSD$  and  $RSA$  are respectively the spectral displacement and acceleration demands corresponding to the maximum localised interstorey drift demand ( $\theta$ ) at a specific limit state (performance state);  $T_0$  is the initial fundamental period of the undamaged structure; and  $\beta$  is the period shift factor that account for period lengthening under inelastic deformation.

It should be noted that the drift related factor, maximum interstorey drift ratio, period shift factor and the fundamental period of the structure used in the equations (2.4) and (2.5) are calibrated from the published experimental results.

Theoretically, the drift factor and period shift factor could be expressed in terms of the maximum IDR provided that the deflected shape of buildings can be reasonably estimated. Following Paulay and Priestley's ductility relationship, one may express the  $\lambda$  and  $\beta$  as follows:

$$\lambda = \frac{3}{2} \cdot \frac{\mu_L}{\mu_G} = \frac{3}{2} \cdot \frac{n\mu_L}{(\mu_L - 1) + n} \quad (2.6)$$

$$\beta = \sqrt{\mu_G} = \sqrt{\frac{1}{n}(\mu_L - 1) + 1} \quad (2.7)$$

Therefore the spectral displacement or acceleration demands for  $\theta$  at a particular limit state is defined given the  $\mu_L$ .

## 2.2. Proposed Ductility Relationships

Improvement to Paulay and Priestley's ductility relationship by considering the mode shape based on the realistic failure mechanism of buildings is proposed. The soft storey failure mode shape as opposed to the assumed linearly varying mode shape is considered in this study.

Since the responses of MI RC buildings are likely to be governed by the 1<sup>st</sup> vibration mode, it is assumed that only the 1<sup>st</sup> mode of vibration is considered. Moreover, this study considers the regular MI RC buildings with uniform storey mass and same storey lateral stiffness with constant yield strength for each storey, which is likely the case for low-rise MI RC buildings without stiffness or geometrical irregularity. In addition, the constant rectangular or triangular external force distributions could be assumed leading to respective global ductilities defined as:

$$\text{Rectangular load distribution: } \mu_G = 1 + \frac{2(\mu_L - 1)}{1 + n} \quad (2.8)$$

$$\text{Triangular load distribution: } \mu_G = 1 + \frac{\mu_L - 1}{n - \sum_{i=1}^{n-1} \frac{(1+i)i}{2N}} \quad (2.9)$$

$$\text{where } N = \frac{(1+n)n}{2} \quad (2.10)$$

## 3. SETUP OF NUMERICAL MODELS

### 3.1. Numerical Models

In this study, 3-, 5-, and 7-storey MI RC building models with a constant storey height of 3m and uniform storey mass of 100 tons except for the roof level of only 70tons were constructed. The weight adopted here are comparable to a 2-bay, 9m by 9m low-rise MI RC building (Zheng *et al.* 2004). Uniform lateral storey stiffness of about 740 kN/mm was adjusted for all three models such that the resulting initial fundamental periods ( $T_0$ ) of structures are consistent with those predicted by Hong and Hwang (2000), Su *et al.* (2003) as shown in Figure 1b. The fundamental periods predicted by the two proposed empirical period-height relationships were found to be consistent with the experimental results of low-rise MI RC, Shear Wall (SW), and Confined Masonry (CM) structures (Lee and Su 2012). Table 1 summarizes some general properties of the models.

Since the effects of axial deformation on MI RC frames and rotational deformation at beam-column joints on overall lateral deformation are negligible due to relatively high rigidity for low-rise MI RC buildings, a simplified 2D lumped mass stick model considering only the translational degree of freedom on each node is simulated as shown in Figure 1a. The Bouc-Wen model (Wen 1976, Ma *et al.* 2004) is incorporated to closely simulate the nonlinear storey restoring force which will be discussed in next session.

The equation of motion of a  $n$ -storey building subjected to earthquake excitations can be represented as (Foliente 1993):

$$\mathbf{M}\ddot{\mathbf{x}} + \mathbf{C}\dot{\mathbf{x}} + \mathbf{R}(\mathbf{x}) = -\mathbf{M}\mathbf{1}\ddot{u}_g + \mathbf{H}' \quad (3.1)$$

where  $\mathbf{M}$  is the mass matrix;  $\mathbf{x}$ ,  $\dot{\mathbf{x}}$ ,  $\ddot{\mathbf{x}}$  are the relative displacement, velocity and acceleration vectors to the ground, respectively;  $\mathbf{C}$  is the damping matrix obtained by assuming a modal damping ratio of 5% for each vibration mode;  $\mathbf{R}(\mathbf{x})$  is the storey restoring force matrix, depending on  $\mathbf{x}$  and other hysteretic

parameters described in Bouc-Wen model;  $\mathbf{1}$  is the unit column vector;  $\ddot{u}_g$  is the ground acceleration;  $\mathbf{H}'$  is the equivalent incremental lateral force vector induced by the P-delta effect.

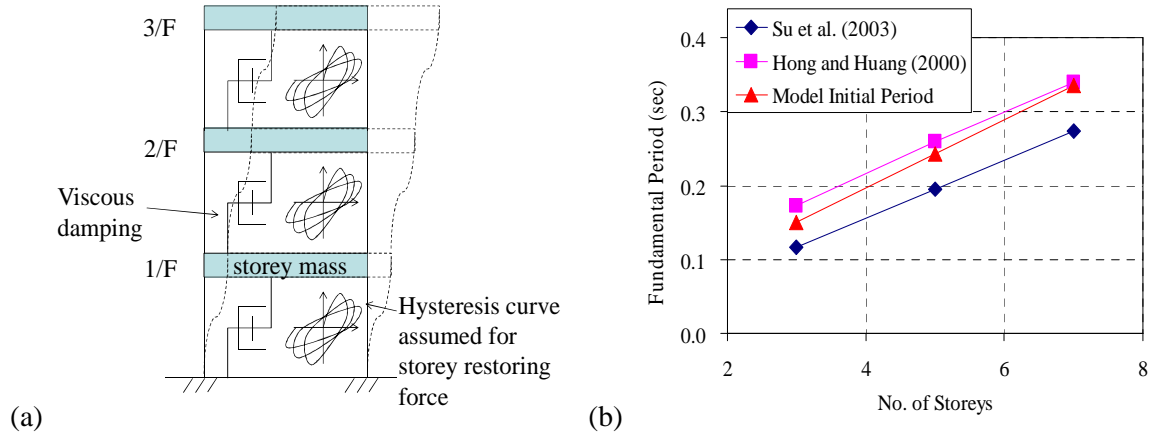


**Figure 1.** (a) 2D lumped mass stick model for MI RC buildings; (b) comparison of model periods to the empirical period.

**Table 1.** Properties of the MI RC buildings models

No. of Storeys, $n$	Building Height (m)	Model Initial Period, $T_0$ (sec)	Base Shear Coefficient at Peak Strength
3	9	0.151	1.0458
5	15	0.243	0.6008
7	21	0.336	0.4214

### 3.2. Hysteretic Model of Storey Restoring Forces

The hysteresis load-displacement curve of MI RC frame structures have been studied extensively by different researchers. Among those, Kakaletsis and Karayannis (2008) tested 1/3 scale single bay and storey masonry-infilled reinforced concrete frame specimens under cyclic horizontal loading, so as to examine the contributions of the types of infill and concentric openings to the force-displacement behaviours. The specimens in same dimensions of 1500 mm width and 1000 mm height were prepared in accordance with current Greece standards similar to Eurocode 2 and 8. For all specimens, infills were designed to have lower lateral strength than the column to avoid brittle frame failure. The specimen IS with strong solid infill mainly failed by sliding of the infill along bed joints was selected for modelling the hysteretic behaviour in this study.

The experimental load-displacement behaviour of specimen IS as well as the numerical hysteresis loops simulated by Bouc-Wen model are presented in Figures. 2(a-b). Bouc-Wen model was used in the study (Wen 1976, Ma *et al.* 2004) to simulate the strength degradation, stiffness degradation and the pinching effects of MI RC wall panels under successive hysteresis loops. The dynamic response was solved by the time-marching scheme using the fourth-order Runge-Kutta integration method. The calibrated parameters that predicted the experimental hysteretic loop with a good accuracy include the initial elastic stiffness  $k = 21.84$  kN/mm, the post-yield elastic stiffness ratio  $\alpha = 0.005$ , and other governing parameters:  $A = 1.0$ ,  $\bar{\beta} = 0.75$ ,  $\gamma = -0.5$ ,  $\bar{n} = 1.0$ ,  $\delta_v = 0.0002$ ,  $\delta_\eta = 0.01$ ,  $\zeta_s = 0.8$ ,  $q = 0.001$ ,  $p = 2.0$ ,  $\psi = 0.2$ ,  $\delta_\psi = 0.002$  and  $\bar{\lambda} = 0.1$ .

The numerical hysteretic model (pattern) was subsequently modified to the elastic storey stiffness in order to simulate storey restoring force under the approximation that the hysteretic storey restoring force is compatible with the experimental results.

In addition, an idealised bilinear restoring force model is further determined as shown in Figure. 3b.

For the lateral displacement ( $\Delta$ ) and interstorey drift ratio ( $\theta$ ) of the model, at the yield state,  $\Delta_y = 7$  mm and  $\theta_y = 0.233\%$ ; at the peak load state  $\Delta_{max} = 15$  mm,  $\theta_{max} = 0.5\%$  and peak strength ( $V_{max}$ ) = 2770kN; at the ultimate state  $\Delta_{ult} = 62$  mm and  $\theta_{ult} = 2\%$ , which the deformability is likely comparable to some of other tested MI RC frames or building models (Mehrabi *et al.* 1996, Kwan and Xia 1996).

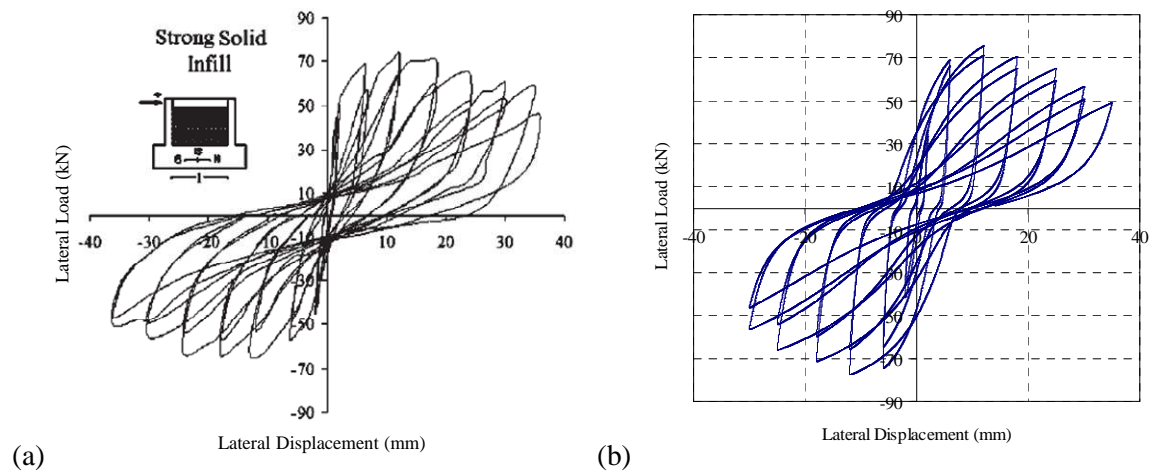


**Figure 2.** Lateral load-displacement hysteresis curves: (a) experimental specimen IS and numerical results; (b) numerical model

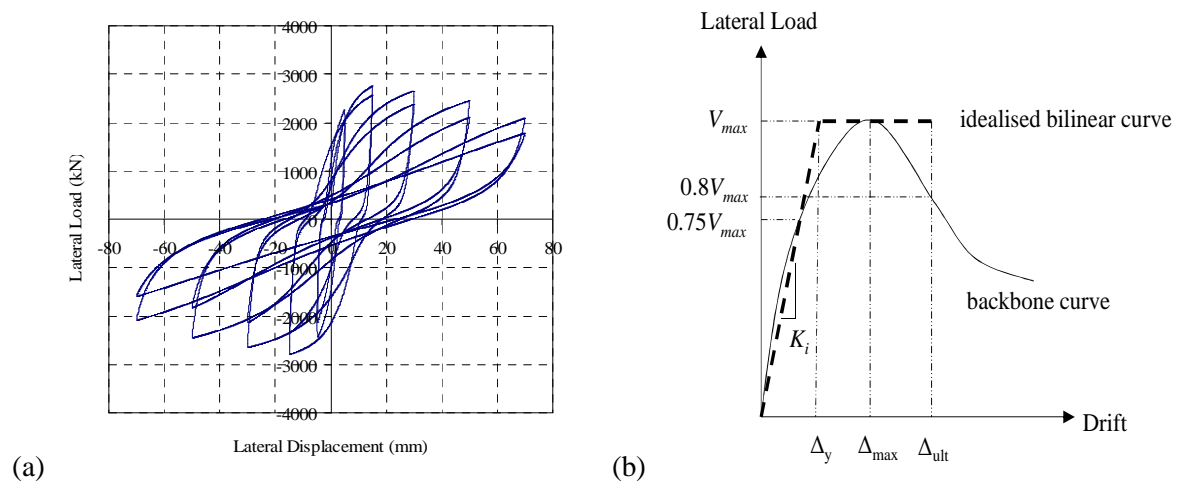


**Figure 3.** (a) Lateral load-displacement hysteresis curve assumed for each storey; (b) idealised bilinear curve for the load-displacement curve

### 3.3. Selected Accelerograms

Incremental dynamic analysis (IDA) was performed to study the seismic response of the three building models subject to 10 different accelerograms, within which 4 accelerograms recorded from strong seismicity regions comprised El Centro, Kobe, Hachinohe and Northridge earthquakes; another 6 set of accelerograms were stochastically generated for low-to-moderate seismicity regions under 2475 return period (RP). The accelerograms considered include far field and near field earthquakes with various characteristic features. Figures. 4(a-d) show the corresponding acceleration response spectra normalized to PGA = 0.5g.

## 4. RESULTS AND DISCUSSION

Incremental dynamic analysis was performed for 3-, 5-, 7-storey MI RC buildings under 10 accelerograms with scaled PGA from 0.2g to 1g with increments of 0.05g to 0.1g. Figures 5(a-c) illustrate the results of ductility correlation calculated from the NTHA, and the predicted ductility

relationship by the three methods discussed previously. The data considered in the following study is limited to local ductility from 1 to 8, which should cover most MI RC frames' actual ductility capacity.

The abbreviations adopted in the figures are as follows: Paulay and Priestley's expression with linear displacement profile in elastic state is denoted by P, while St refers to the correlation derived from simple static PO analysis using triangular loading distribution. Similarly, Sr refers to the one with rectangular loading distribution. NLa, NLb, NLc, NLd refer to the NTHA ductility relationship calculated from different sets of input accelerograms with the same categories defined in Figures 4 (a-d).

In general, consistent trends between the local and global ductilities from IDA are observed. The three methods for predicting the ductility relationship are likely capable of estimating the actual trend, with some being performing better at specific MDOF. The average of absolute percentage error for each prediction method is illustrated in Table 2. Paulay and Priestley's prediction shows superiority to others for 3-storey buildings, while triangular load method generally provides the best overall accuracy to the prediction to 3-, 5-, 7-storey buildings with average absolute percentage errors limited to about 8 to 13%. The details of results are interpreted in the followings.

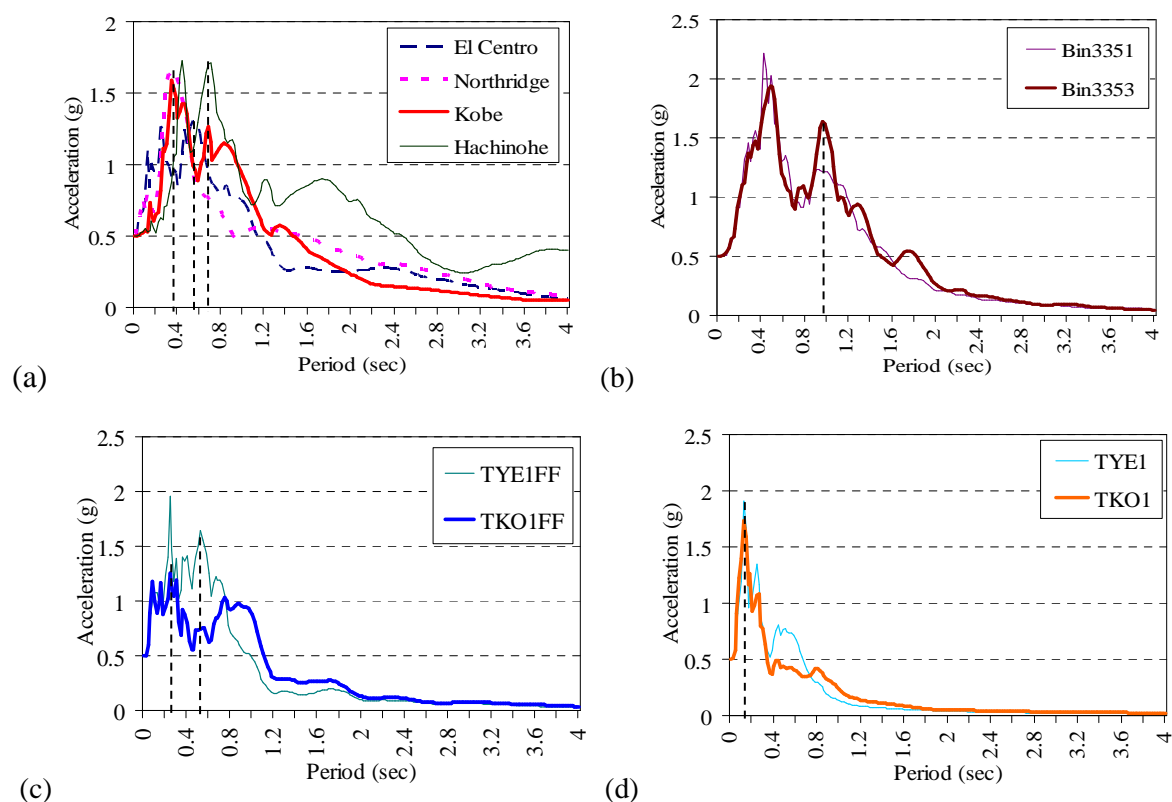


**Figure 4.** Normalized acceleration response spectra at 0.5g for selected accelerograms: (a) from high seismicity regions; stochastically generated accelerograms from low-to-moderate seismicity regions (b),(c) at far field soil site, and (d) at near field soil site.

#### 4.1. Comparisons of Different Ductility Prediction Relationships

Linear ductility correlation is predicted by all three methods for ground floor soft storey buildings, as stated in Equations 2.3, 2.8, and 2.9. The local ductility always tends to be larger than the global ductility due to deformation concentration on the weak storey. It coincides with the similar findings by Gupta and Krawinkler (2000) for larger maximum interstorey drift ratio than the roof drift ratio.

Predicted global ductilities by three methods match at local ductility factor = 1, while their differences increase with local ductility. The global ductility obtained by rectangular load distribution is found to

be the largest, while the Paulay and Priestley's ductility curve estimates the lowest global ductility. It is suggested by the slope of the correlation in the prediction equations, which is due to the differences between the yielding deflected shapes assumed in the theoretical PO models.

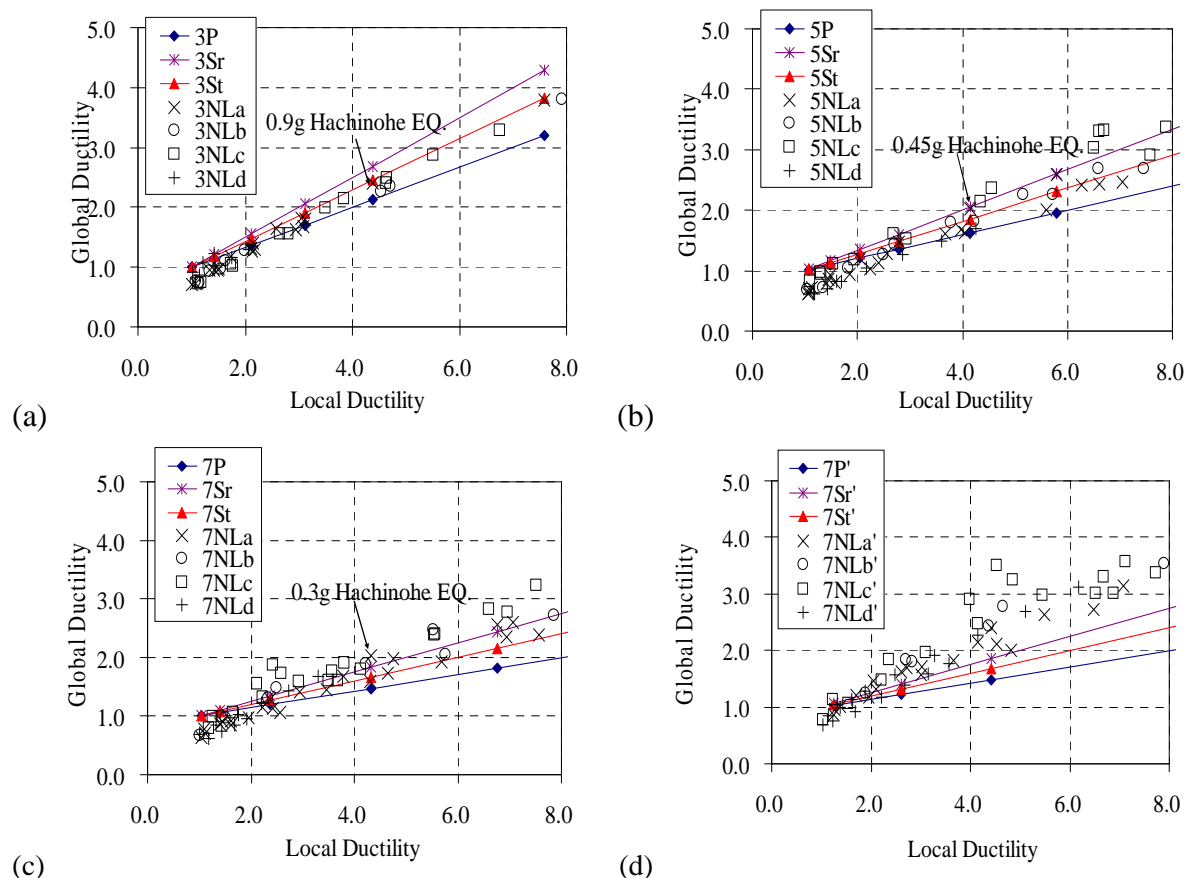


**Figure 5.** Local ductility against global ductility from NTHA and prediction curves: (a) 3-storey, (b) 5-storey, (c) 7-storey; (d) 7-storey building using initial undamaged elastic stiffness for bilinear idealisation.

**Table 2.** Absolute percentage error for the ductility prediction curves.

No. of Storeys	Paulay and Priestley (1992) (P)	Rectangular load (Sr)	Triangular load (St)
	average (%)	average (%)	average (%)
3	6.87	16.69	7.78
5	13.95	14.48	10.34
7	19.93	10.15	12.71

Excluding data with local ductility factor < 2, to avoid distorted % from low global ductility factor.

#### 4.2. Effect of Soft Storey Assumption against no. of Storeys

As shown in Figures 5(a-c), the results obtained by the NTHA tend to be higher than the predicted curves with the increasing number of storeys, especially for 7-storey buildings. Since the predicted curve is based on first storey yielding assumption, it may not be valid for high rise buildings with more storeys which are likely to be excited to higher vibration modes.

The above observation can be proved by the storey displacement envelopes from NTHA. For instance, 3-, 5-, 7-storey buildings being excited to a similar local ductility demand of about 4 to 4.5 could be compared (0.3g Hachinohe earthquake for 7-storey, 0.45g for 5-storey, 0.9g for 3-storey building as shown in Figures 5(a-c)), i.e. the maximum first storey drift was excited to about 28 to 31.5 mm. Besides other storey levels being within yield displacement limit of 7 mm, the maximum interstorey drifts of the 2<sup>nd</sup> floor for 3-storey and 5-storey were excited to 7.5 mm and 12.7 mm respectively,

while those for the 2<sup>th</sup> and 3<sup>rd</sup> floors of 7-storey building were about 17.4 mm and 10.6 mm respectively. It suggests the underestimation of the predicted curve is probably due to the invalidity of the 1<sup>st</sup> floor soft storey assumption for buildings with significant yielding occurred in upper storeys under the higher mode effects.

FEMA 440 suggests that the use of equivalent SDOF system to characterize the nonlinear behaviour of a system is not appropriate when higher mode effects are non-trivial or the static PO analysis cannot reflect the inelastic mechanisms. The IDR derived from first modal PO analysis is prone to be inaccurate under increased storey levels or fundamental period of buildings, as tortuous higher mode shapes have a significant contribution to the interstorey drifts. Iwan *et al.* (2000) have found that the higher mode contribution is negligible when the building's periods are shorter than the ground pulse duration, while the long period structure under large displacement and velocity pulses of near field earthquakes is likely to have higher mode participation. Simply comparing the fundamental undamaged period of the buildings in Table 1 to the 1<sup>st</sup> corner period of the accelerograms in Figure 4, defined here as the largest period corresponding to the plateau in RSA, it can be observed that the 1<sup>st</sup> corner periods of accelerograms mainly lie within 0.4-0.7 sec with a few lying in about 0.2 sec for the near field earthquake or 1 sec for far field soil sites. Hence, with the consideration of the period lengthening effects after structural damage, the fundamental period of 7-storey buildings with an initial value of around 0.36 sec is likely to exceed the 1<sup>st</sup> corner period of some of the accelerograms, resulting to higher possibility of higher mode participations as suggested by Iwan *et al.*

### 4.3. Bilinear Idealisation of Load-displacement Curve

The results shown so far are based on the idealised bilinear model defined in Figure 3(b). Under the range of ductility considered, idealisation by adjusted  $K_i$ , secant stiffness to the 75% peak strength, results to better approximation of the actual load-displacement behaviour of the storey in NTHA. The effects of different bilinear idealisation model on the ductility correlation are shown in Figure 5(d), which undamaged initial elastic stiffness ( $K_0$ ) is assumed for 7-storey building model. Both the local and global ductilities estimated from the NTHA results by using  $K_0$  will result in overestimation. Under the uniform storey stiffness model studied, the yield storey and roof displacement will be underestimated by the same factor, and so is the overestimation of local and global ductilities.

Another observed phenomenon is the likely underestimation of global ductility for local ductility range from 1 to 2. It could be due to the overestimation of the yield roof displacement in PO models due to the adjusted and softened storey stiffness  $K_i$  assumption for all storeys, in which the upper storeys under small interstorey deflection are likely to remain as its undamaged elastic stiffness.

## 5. CONCLUSION

The findings from this study can be summarized as follows.

1. For 3-, 5-, 7-storey low-rise MI RC buildings with soft storey mechanism considered in this study, a linear local and global ductility relationship can be satisfactorily drawn by static PO provided that bilinear idealisation of the storey load-displacement behaviour can be reasonably approximated.
2. Due to the participation of higher modes, the higher the degree of nonlinearity and the number of storeys are, the larger the discrepancy of the predicted ductility to the actual one becomes.
3. MI RC frame model calibrated against the single bay and storey specimen is assumed for the storey load-displacement relationship. The ultimate drift capacity of the tested specimen could be relatively high comparing to some MI RC frames under low aspect ratios, high axial loading and strong infill that exhibits brittle frame failure. Other models accounting this load-displacement behaviour are necessary to draw a more rigorous conclusion on the ductility relationship.
4. Three compact expressions of ductility relationships are provided to account for three different initial yielding shapes, with the triangular load distribution being superior for overall average absolute error of less than 13% for local ductility ranging from 2 to 8.

5. The ductility relationships verified herein can possibly be used for calibration of drift factors and period lengthening factor up to 7-storey buildings despite scarcity of experimental data.

#### ACKNOWLEDGEMENT

The authors would like to thank Dr. H.H. Tsang and final year undergraduate Victor Ma for providing the stochastically generated accelerograms for analysis.

#### REFERENCES

- ATC (1996). ATC-40, *Seismic Evaluation and Retrofit of Concrete Buildings*, Vols. 1&2, Applied Technology Council (ATC), Redwood City, California, USA.
- Federal Emergency Management Agency (FEMA 356), 2000. *Prestandard and Commentary for the Seismic Rehabilitation of Buildings, Report FEMA 356*, Washington D.C., USA.
- Federal Emergency Management Agency (FEMA 440), 2005. *Improvement of Nonlinear Static Seismic Analysis Procedures, Report FEMA 440*, Washington D.C., USA.
- Foliente, G.C. (1993). Stochastic Dynamic Response of Wood Structural Systems. *Ph.D. Thesis*, Virginia Polytechnic Institute and State University, Blacksburg, Virginia.
- Gupta, M. and Krawinkler, H. (2000). Estimation of Seismic Drift Demands for Frame Structures. *Earthquake Engineering and Structural Dynamics* **29**(9), 1287-1305.
- Hong, L.L. and Hwang, W.L. (2000). Empirical Formula for Fundamental Vibration Periods of Reinforced Concrete Building in Taiwan. *Earthquake Engineering and Structural Dynamics*, **29**(3), 327–337.
- Iwan, W.D., Huang, C.T., and Guyader, A.C. (2000). Important Features of the Response of Inelastic Structures to Near-field Ground Motion. *Proceedings of the 12th World Conference on Earthquake Engineering*, New Zealand Society for Earthquake Engineering, Upper Hutt, New Zealand, Paper No. 1740.
- Kakaletsis, D.J. and Karayannis, C.G. (2008). Influence of Masonry Strength and Openings on Infilled R/C Frames Under Cycling Loading. *Journal of Earthquake Engineering* 2008; **12**(2), 197-221.
- Kwan, A.K.H. and Xia, J.Q. (1996). Study on Seismic Behavior of Brick Masonry Infilled Reinforced Concrete Frame Structures. *Earthquake Engineering and Engineering Vibration*. 16(1), 87-98. (In Chinese)
- Lee, C.L. and Su, R.K.L., (2012). Fragility Analysis of Low-rise Masonry In-filled Reinforced Concrete Buildings by a Coefficient-based Spectral Acceleration Method. *Earthquake Engineering & Structural Dynamics*, **41**(4), 697-713.
- Ma, F., Zhang, H., Bockstedte, A., Foliente, G.C., Paevere, P. (2004). Parameter Analysis of the Differential Model of Hysteresis. *Journal of Applied Mechanics, ASME*, **71**(3), 342-349.
- Mehrabi, A. B., Shing, P. B., Shuller, M. P., and Noland, J. L. (1996). Experimental Evaluation of Masonry-infilled RC frames. *Journal of Structural Engineering*, **122**(3), 228–237.
- Miranda, E. (1999). Approximate Seismic Lateral Deformation Demands in Multistory Buildings. *Journal of Structural Engineering*, **125**(4), 417-425.
- Paulay, T. and Priestley, M.J.N. (1992). *Seismic Design of Reinforced Concrete and Masonry Buildings*. John Wiley & Sons, Inc., USA.
- Ruiz-García, J. and Negrete, M. (2009). A Simplified Drift-Based Assessment Procedure for Regular Confined Masonry Buildings in Seismic Regions. *Journal of Earthquake Engineering*, **13**(4), 520-539.
- Su, R.K.L. and Zhou, K.J.H. (2009). Inherent Strength-based Approach for Collapse Seismic Assessment of Low-rise Masonry Buildings. *Proceedings of 2009 NZSEE Conference*, Christchurch, New Zealand, 3-5 Apr 2009, 35-42.
- Su, R.K.L., Chandler, A.M., Lee, P.K.K., To, A.P., and Li, J.H. (2003). Dynamic Testing and Modelling of Existing Buildings in Hong Kong. *Transactions of Hong Kong Institution of Engineers*, **10**(2), 17–25.
- Su, R.K.L., Lee, C.L. and Wang, Y.P. (2012). Seismic Spectral Acceleration Assessment of Masonry in-filled Reinforced Concrete Buildings by a Coefficient-based Method. *Structural Engineering and Mechanics*, **41**(4), 1-16.
- Su, R.K.L., Lee, Y.Y., Lee, C.L. and Ho, J.C.M. (2011). Typical Collapse Modes of Confined Masonry Buildings under Strong Earthquakes. *The Open Construction and Building Technology Journal*, **5**(Suppl. 1-M2), 50-60.
- Wen, Y.K. (1976). Method for Random Vibration of Hysteretic Systems. *Journal of Engineering Mechanics Division, ASCE*, **102**(2): 249-263.
- Zheng, S.S., Yang, Y. and Zhao, H.T. (2004). Experimental Study on Seismic Behavior of Masonry Building with Frame – Shear Wall Structure at Lower Stories. *China Civil Engineering Journal*, **37**(5), 23-31.